Available online at www.sciencedirect.com

ScienceDirect

Current Opinion in
Colloid & Interface Science

Quantitative light microscopy of dense suspensions: Colloid science at the next decimal place

Brian D. Leahy[a,b,1], Neil Y.C. Lin[a,b,1], Itai Cohen[a,*]

Since the days of Perrin (1908) [1], microscopy methods have played an important role in the study of colloidal suspensions. Along with the continued development of new imaging techniques, colloid scientists have also implemented a sophisticated range of computational analyses. These analysis techniques are often the unsung heroes that hold the promise of unlocking scientific mysteries at the next decimal place of colloid science. They now enable precision measurements of particle location and size (Bierbaum et al., 2017; Kurita et al., 2012) as well as measurements of local stresses and forces (Lin et al., 2016). Here, we spotlight these exciting advances focusing on the analysis of simple brightfield and confocal microscope images of dense colloidal suspensions as well as the scientific mysteries they may unravel.

Address
[a] Department of Physics, Cornell University, Ithaca, NY 14850, United States
[b] School of Engineering and Applied Sciences, Harvard University, Cambridge, MA 02138, United States

[*] Corresponding author.
(ic64@cornell.edu)

Keywords:
Colloidal suspensions
Microscopy
Imaging
Forces
Measurement science

Current Opinion in Colloid & Interface Science (2018) **34**, 32–46
This review comes from a themed issue on **Microscopy Methods**
For a complete overview see the issue and the Editorial

Article History:
Received 10 December 2017
Received in revised form 12 March 2018
Accepted 13 March 2018
Available online 23 March 2018

https://doi.org/10.1016/j.cocis.2018.03.002

1. Introduction

> "Why should one wish to make measurements with ever increasing precision? Because the whole history of physics proves that a new discovery is likely to be found lurking in the next decimal place."
>
> [(Floyd K. Richtmyer, 1931) [5]]

Look through a colloid scientist's microscope and you'll find an amazing array of phenomena that scientists and engineers investigate with colloidal suspensions. Particles entropically assemble into a zoo of crystal structures [6–11]. Aided by patterned substrates [12,13], gel coatings [14], depletion interactions [15–20], charge induced interactions [21–23], magnetic interactions [24–26] and DNA programmable interactions [27–30] the variety of accessible structures that suspensions form is breath taking. Active colloidal particles jet around, providing fertile testing grounds for far-from-equilibrium physics [31–36]. The behaviors of liquids [37,38], interfaces [39], gels [17,40,41] and glasses [42–47] are resolved with fine detail. Confocal rheoscopes illuminate the structural underpinnings of rheological behaviors from thixotropy [45,48,49] to shear thickening under confinement [50]. And the particles are no longer just spheres [51]; particle shapes have blossomed into a beautiful set of rods [52], clusters [24,53], dimers [54], lock-and-key particles [55], and even designed shapes from pentagons to letters [56–59], with simulations promising new materials from many of these shapes [60].

Simple microscopy methods such as brightfield and confocal are a large reason for the continued excitement in exploring such colloidal phenomena. The particles' large, micron-scale size and slow, millisecond- to second-scale dynamics allow key behaviors to be easily investigated by microscopy [19,44,46,61–65]. A modern microscope can image thousands of particles in a blink of an eye, and simple automated software routines can locate these particles to within 30 nm, while missing only a few percent of the

particles [66–68••]. Importantly, microscopy allows for local measurements of a suspension. Since particle interactions are often short ranged, the suspensions are frequently heterogeneous, and it is difficult to apply mean field concepts to understand their bulk behavior. Thus, the ability to image the local suspension structure has catalyzed a growth in the field, as theories that link local structures and their dynamics to the bulk suspension behavior can be tested on a per-particle level with statistically robust and well-controlled samples.

Yet some of the most interesting physical phenomena in colloidal science are not testable with traditional microscopy techniques. In typical experimental configurations, colloidal particles only deviate from hard-sphere interactions at nanometer separations. Numerous pioneering studies have elucidated how particle pairs interact at short distances [69–72]. However, measuring the strength of these interactions in dense suspensions, is difficult with the 30-nm localization accuracies of typical microscopy methods. For particles interacting *via* longer-range depletion forces, which occur on the 50–100 nm range, the bond energy can change greatly over the 30 nm uncertainty of typical approaches. Accurate localization is even more important for advancing studies of non-equilibrium colloidal matter, such as glasses and gels. Here, small changes in interparticle spacing can have huge effects on the macroscopic physics – a slightly tighter cage in a glass will have a much longer relaxation time, two particles slightly farther apart in a gel might no longer be bonded together. Worse, these systems are fundamentally heterogeneous, so there is little hope of inferring local properties of the material from scattering and bulk measurements. Moreover, since even the most monodisperse suspensions are not perfectly homogeneous [3], there is no guarantee that forces, stresses, or viscosities are homogeneous. Bulk methods such as rheometry cannot measure these local variations, while traditional microscopy cannot measure these mechanical properties at all. Finally, as particles with more complicated structure start to be synthesized more readily, it will become increasingly important to determine how these local properties depend on particle shape and size.

But over the past decade the situation has changed. With the advent of modern imaging techniques, faster computers to analyze the data, and the synergistic combination of the two, new techniques have been developed that are paving the way for a renaissance in the study of colloid suspensions. Today, research groups regularly acquire three-dimensional images of colloidal suspensions in real time. Coupled with careful analysis, these images provide a vast amount of information, yielding everything from nanometer-accurate position and size measurements [2••], shape information and orientation about non-spherical particles [52,73,74••], to even super-resolution images of individual particle microstructure [75•,76]. Just as exciting, researchers have found ways to use microscopes to measure stresses [4••], forces [77], and moduli [4••,78••]. Such techniques promise to fundamentally alter the toolbox available to scientists investigating suspensions.

In this article we highlight some of the more recent advances in the *analysis* of confocal and light microscopy images of dense colloidal suspensions. Such analyses have had an enormous impact on colloid science but have received less attention than developments in microscopic imaging. There have, of course, been many exciting developments in microscopy over the past decade. For instance, there have been amazing developments in super-resolution imaging techniques including photoactivated localization microscopy (PALM) [79], stochastic optical reconstruction microscopy (STORM) [80], and stimulated emission depletion (STED) [81], as well as the continued development of ever more powerful techniques ranging from structured illumination [82] to lattice-light sheet [83] and Bessel Beam microscopy [84]. Another new set of techniques to keep an eye out for is holographic microscopy. While the idea of holography is old [85,86], recent improvements in the analysis of digital holograms have catapulted holography to the cutting edge of colloidal microscopy methods. For dilute suspensions, holography provides particle position, size, and even refractive index and shape with nanometer accuracy, from images captured with millisecond time resolution. Holographic microscopy excels for imaging single spheres [87–92•], clusters of spheres [93–95], rodlike colloidal particles [96,97], and even individual tracer particles in an otherwise un-imaged dense suspension [98•]. It can even be done on the cheap [99]. However, current methods are not yet able to accurately analyze holographic images of dense suspensions. As such, the application of holography to analyzing dense colloidal suspensions awaits further developments. Our focus on image analysis is based partly on practical criterion of space, but it is also based on a philosophical underpinning: New microscope imaging techniques can be expensive, whereas computers are cheap. Microscopes are costly to duplicate and require extensive maintenance, whereas software is easy to transfer from machine to machine and is practically maintenance-free. Why spend money buying new microscopes and complicated optics when you can improve the data you already have with better *inference* from the same images and analysis techniques that enable new science?

2. Better Inference

Since the landmark work by Crocker and Grier in the 1990s [66], colloidal science has relied heavily on automated particle tracking. The original Crocker-Grier routines in IDL can readily locate thousands of particles in microscope images and link the particles' trajectories through time, all in a few seconds. The ability to measure thousands of individual particle positions and to track those particles through time enables the testing of detailed microscopic theories, which has had a profound effect on colloidal science. It is because of particle tracking that we can visualize how crystals form and melt [62], understand how glasses rearrange and relax [44], and investigate the patterns formed in coffee rings as they dry [100]. Just as important, these particle tracking routines are easy to use, requiring no equipment other than a computer and an ordinary microscope, and requiring little extra training.

2.1. Centroid identification and related methods

The original particle location algorithm of Crocker and Grier [103] is now more than two decades old and still finds massive usage. Its permanence and effectiveness is due in a large part to its simplicity: it identifies particle positions as the intensity centroid of bright regions in an image. And due to its extensive usage, the original routine has been improved greatly by many people over the past two decades. Researchers have layed out how to take the best images for particle tracking [67,104]. Sources of bias, such as from anisotropic preprocessing kernels [105] or pixel bias [106–108•], have been identified and diminished. Extensions to the algorithm can identify nearly all the particles in a field of view [68••]. And, inspired by the original method, other algorithms have sprung up that can rapidly identify particle centers with little bias [109] or even for identifying particles that are not spheres, with shapes from rods to triangles being located [52,73,74••,110,111].

However, the original Crocker-Grier method struggles with measuring particle sizes, and it has difficulty in measuring particle positions in size-polydisperse suspensions. Most particle location algorithms, including the method of Crocker and Grier, start by smoothing the image with a Gaussian blur to accentuate the particles (blob detection). But the optimal smoothing kernel size is tricky to find – use too small of a kernel and the image will be too noisy, use too big of a kernel and the particles will be blurred out into nothingness. Even worse, for samples with significant size polydispersity, an optimal kernel size might not exist. Leocmach and Tanaka [101] circumvent this problem of finding the correct kernel size by filtering the image repeatedly on many scales, a technique from computer vision known as a Scale Invariant Feature Transform or SIFT. Processing the image on a range of scales both enables particle identification in suspensions with polydisperse sizes and provides a way to measure the particle radii – the particle radius is the size at which the filter produces the maximal response (Fig. 1a–b). By using this technique to measure particle size in a size-polydisperse suspension, Leocmach and Tanaka [101] were able to measure the coupling between structural heterogeneity and particle size in super-cooled liquids (Fig. 1c), and they were able to show that smaller particles are expelled out of growing crystallites. However, while the method provides good relative sizing, it needs external calibration to give absolute particle radii measurements.

A conceptually similar approach is employed by Brujic et al. [112] to measure particle size. Rather than using SIFT by convolving the image with a Gaussian blob over a range of scales, Brujic et al. use deconvolution, by repeatedly deconvolving the image with the kernel of a sphere over a range of sphere radii. Since an image of a sphere can be viewed as a delta-function at the sphere's position convolved with a spherical kernel, the deconvolution of the image with a spherical kernel produces a series of spikes at the spheres' locations. This method gives the sphere's radii as well – the sphere's radii can be identified with the kernel whose radius produces the strongest response. Using this approach, researchers have been able to characterize force networks and distributions [112] and the number of excess contacts [113] in jammed emulsion droplets.

But the most exciting new improvements to inference from images go beyond treating the particles as fuzzy bright blobs on the camera. Instead, they use additional information that the experimentalist knows about the image and the sample to greatly improve measurements of the recorded colloidal particles.

2.2. Inferring radii from positions

One such approach is to assume something about the relation between images over time. Combining fast but comparatively uninformative analysis methods, such as centroid-finding for particle positions, with a secondary analysis can not only increase precision, but can even provide new information.

A prime example of this idea is using only the measured particle positions to infer the particle radii [3,114]. Since approximate particle positions can be measured quickly, easily, and robustly, this inference technique provides a rapid way to back out individual particle radii. The algorithm infers the particle radii by assuming that the time-average surface-to-surface separation of one particle is the same as the time-average surface-to-surface separation in the entire sample. By tracking the center-to-center separation distance of all the particles in the image over time, and using the known sample-average surface-to-surface separation, Kurita and Weeks [3] can infer the individual particle radii from a time series (Fig. 1d). While it is not clear how good the assumption of equal separations is in general, Kurita et al. [3] have shown that the algorithm produces accurate results when fed simulated positions, such as positions of particles in a roughly monodisperse suspension, particles in a roughly bidisperse suspension, randomly-close-packed particles, and even of particles in a colloidal gel. In addition, they show that the experimentally measured radii distributions determined from their inference conform to a directly-measured size distribution from holography (Fig. 1e). From simulation data, they show that their indirect inference method can measure particle radii with an accuracy of either 0.5% of the particle's radius or 15% of the radii polydispersity, whichever is greater. Using these and related radii inference methods, researchers have shown that nucleation in 3D colloidal crystals tends to happen in regions of exceptionally high monodispersity [3], large particles in colloidal glasses have slower dynamics [115•], and jammed suspensions of hard [114] or soft [102•] spheres are hyperuniform (Fig. 1f).

While inferring particle radii solely from measured positions is rapid and easy to apply to existing datasets, its applicability is limited to systems where the assumption of equal average separation is valid. The original version of the algorithm assumes that the experimentalist knows the neighbor-averaged surface-to-surface separation, and that the average separation is the same for all particles on the time scale of the time series. In addition, the inferred radii could be biased if the errors in particle positions are

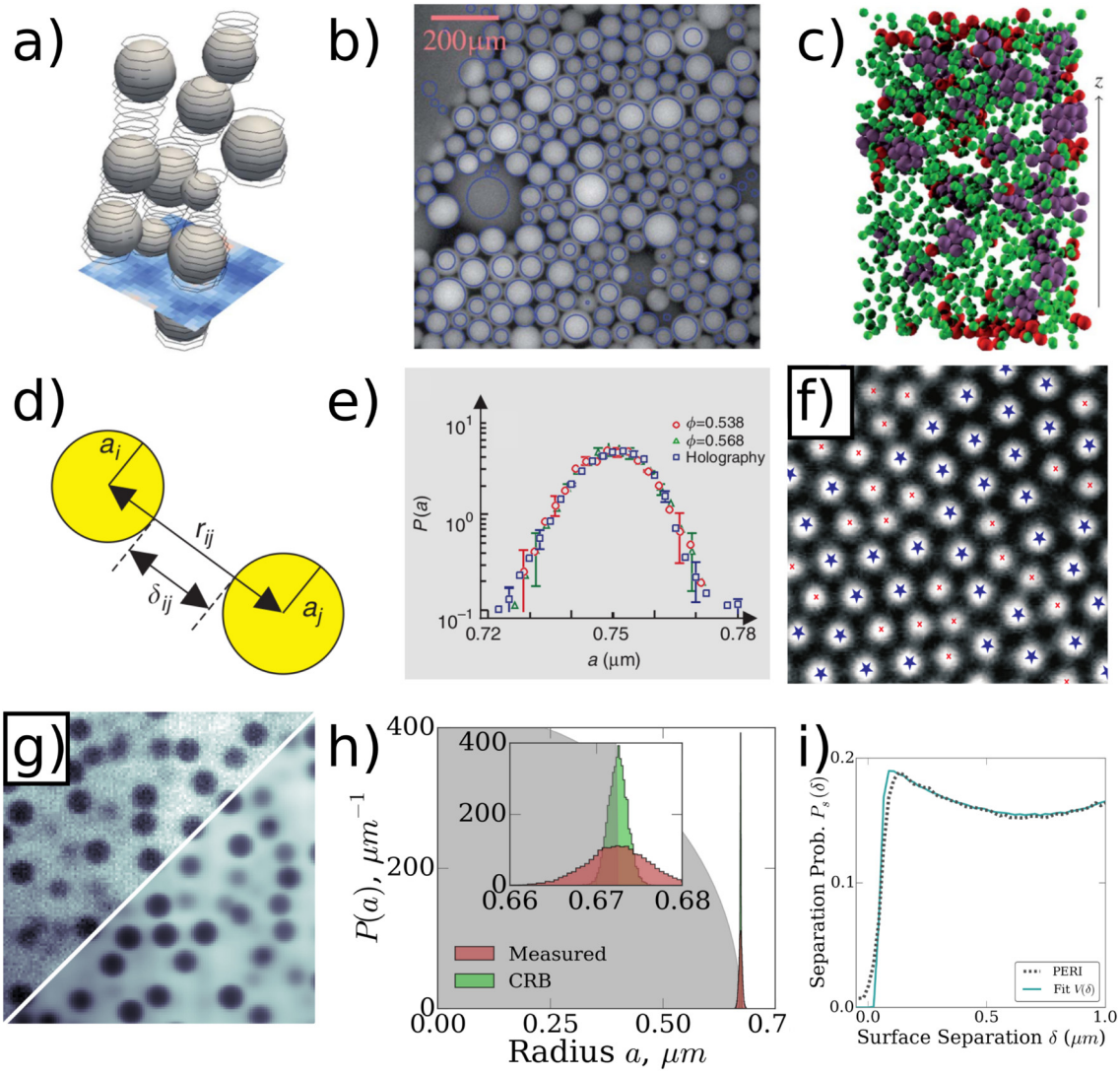

Fig. 1 Additional inference from images. *Multiscale method:* The multiscale method finds particle radii by the response to blob detection over a series of scale (a), which allows direct measurement of particle sizes (b). By looking at particle size distributions in a supercooled liquid (panel c), Leocmach and Tanaka showed that local icosahedral ordering (purple particles) centers around smaller (green) particles, and that crystal-like regions (red particles) do not occur near smaller particles. Adapted from ref. [101]. *Inferred Radii:* An alternative method to finding particle radii is to infer them from particle separations over a time series of images, assuming the average particle separation is the same throughout the sample (d). This provides easy access to particle radii, as shown by the agreement in particle size distributions compared to holography (e). By using this and similar methods, Dreyfus et al. were able to accurately measure hyperuniformity in jammed suspensions of size-bidisperse soft spheres (panel f, small and large particles as red and blue markers, respectively). Adapted from refs [3,102•]. *PERI:* PERI measures particle properties by generating a complete reconstruction of the entire image (panel g, raw data on left and reconstruction on right). The fitted parameters in the reconstruction provide accurate particles measurements, including particle radii to 3 nm (h). The accuracy is good enough to measure nm-scale interaction potentials (i).

correlated with the particle separation, which is the case for simple methods such as centroid-finding that do not account for blurring of the point-spread function. As such, inferring particle radii from the positions is best suited for long time series of homogeneous suspensions.

2.3. All the information

When extremely accurate measurements of particle positions and radii are needed for individual images, the most exact technique is PERI, or Parameter Extraction from Reconstrucing

Images [2••]. PERI operates by fitting the image to a detailed, physically accurate, *in silico* model of the sample and the optical train, which creates a reconstruction of the entire image (Fig. 1g). Once the model, which includes everything from particle positions and sizes to aberrations in the microscope lens, accurately fits the experiment image, the fitted parameters are read out to get highly accurate inference on particle positions and sizes. In fact, when the physical model is complete and correct, PERI extracts *all* the useful information from the image: the unexplained portion of the data is only photon shot noise and the electronic noise of the detector. PERI can readily analyze three-dimensional images of thousands of particles, locating each and every particle's *position and radius* with accuracies of 1–3 nm in typical imaging conditions (Fig. 1h). By correctly accounting for optical diffraction and uneven illumination in the image, PERI can analyze images of dense suspensions without the significant bias present in other analysis techniques. The data are clean enough to measure interparticle interactions with a 10 nm range, even in a size-polydisperse suspension of spheres (Fig. 1i) tebierbaum2017light. While the principle of PERI is general, it is currently only implemented for confocal images of colloidal particles, regardless of volume fraction.

The power of PERI comes at a price in computer time and user knowledge. While traditional methods for identifying particles, such as centroiding, can analyze a 3D image in a few seconds, PERI can take from 1 to 24 h to fit a complete image. Analyzing a time series of a few thousand separate images quickly becomes impractical on a single desktop computer. Fortunately, since the images are analyzed independently, this process is easily undertaken for each image in parallel on a cluster or supercomputer. With the advent of cheap cloud computing platforms such as Amazon Web Services, a researcher can spawn hundreds of processes at pennies on the compute-hour, allowing rapid and easy analysis of separate time series. Additionally, PERI works best when the microscope's optical train is accurately described. It remains to be seen how robust a given description of the optical train is across different microscopes and imaging variations. If the microscope's optical train is not well described by PERI, then the user will have to spend a considerable amount of time implementing a detailed model of the microscope. Hopefully, as PERI matures these questions will be answered.

We provide a comparison of the aforementioned inference techniques in Table 1. While this list of particle position inference methods is by no means complete, it highlights some of the exciting developments and the range of analysis capabilities that are now readily accessible.

3. Using light microscopy to measure forces & stresses

This next decimal of precision in image analyses is also opening the door to measuring forces at the single particle scale. This capability is, in turn, enabling profound new scientific discoveries in colloid science. As a community we are now poised to understand in unprecedented detail how colloid based materials respond and evolve microscopically when they flow, yield, crack, creep, or even fracture.

Until recently, measurements of force and stress distributions were inaccessible in light or confocal microscopy of dense suspensions. Instead, microscopy has mainly been used to characterize the local suspension structure using, for example, pair correlation functions and various order parameters (Ψ_6, Ψ_4, *etc.*) as well as particle motions ranging from simple diffusion to cage hopping [44]. While these pioneering measurements have provided fruitful information about colloidal materials in liquid, crystal, glass, and gel phases, many scientific questions and debates remain because of the lack of information related to force distributions in these suspensions. Recently, however, new avenues for measuring such force and stress distributions have become available, through techniques such as local strain measurements, boundary stresses measurements, Stress Assessment from Local Structure Anisotropy (SALSA), phonon modes analyses, and microrheology. The underlying methodology of these techniques can be roughly divided into two categories: analysis based on elastic linear response (strain measurements and boundary stress microscopy) and statistical mechanics approaches (SALSA, phonon mode, and microrheology). Because of their different working mechanisms, these

Table 1 Comparison of inference methods for microscopy images.

	Centroiding [103,116,117]	Multiscale detection [101,118]	Inferred radii [3]	PERI [2••,119]
Analysis time	1 s	10 s	Not listed	1–24 h
Parallel computing?	Yes	Yes	No	Yes
Positional Accuracy	10–30 nm	~30 nm	n/a	1–3 nm
Radii accuracy	n/a	~0.1R	≲10 nm	3 nm
Assumptions	Qualitative	Qualitative	Long-time imaging, radii don't change	Optical train accurately described
Strengths	Simple and rapid	Simple relative radii measurement	Fast R	Highly accurate x, y, z, R measurement
Drawbacks	Inaccurate for dense suspensions	Calibration needed for absolute radii measurement	Radii & positional errors coupled	Long analysis time
Open source?	Yes	Yes	No	Yes

methods can also be used in combination to back out forces due to Brownian, hydrodynamic and contact interactions, as well as suspension viscosities [48,120•], and moduli [4••,78••].

3.1. Strain measurements

All solids display highly heterogeneous deformation fields when they yield. Therefore, understanding the local deformation or strain tensor and how it evolves under external loads is important to elucidating the nonlinear response of materials. The strain measurement technique calculates the local strain at a central particle from the neighboring particle displacements [5,47,63,121,122,133,134•,135–137]. The determined strain can then further be separated into affine and non-affine deformations. The non-affine part of the strain is critically relevant to the nonlinear response in yielded materials. The strain measurement technique has been used to study the defect nucleation dynamics in colloidal crystals [63], and the yielding mechanisms in glasses with specific focuses on the shear transformation zone [47,122,135] and Eshelby inclusions [121,122] (Fig. 2a). Importantly, however, the absolute strain relative to an undeformed lattice or configuration can only be determined for a crystalline suspension. Moreover, only the affine response can be related to the stress *via* a measurement of the modulus. In liquid or glassy suspensions the situation is further complicated by the fact that only relative strains are calculated. Whether these relax or further concentrate local stresses is difficult to interpret from experimental measurements of the strains alone.

3.2. Boundary stress microscopy

The mechanical response of soft materials can be highly heterogeneous. Measuring such spatial fluctuations of forces can provide valuable insights into the mechanisms that give rise to the extraordinary strengths of amorphous systems. Unfortunately, conventional microscopic flow measurements are only able to report the response that is averaged over a large area, glossing over many important microscopic features. Boundary stress microscopy however, visualizes these intriguing force patterns at the sample boundary [123••,124••] (Fig. 2b). This method shares the same principles as traction force microscopy but is applied to dense suspensions. Here, a thin layer of elastomer with embedded tracer particles is attached to the plate of a shear device (*e.g.* a rheometer or custom-made shear cell). When the loaded sample is sheared, its shear stress is then transmitted to the boundary and deforms the elastomer. By measuring the displacement of the tracer particles and the elastomer storage modulus, one can determine the spatial variation of the stress on the boundary. The main difference in philosophy with traction force microscopy is the focus on large surface regions and characterization of the inhomogeneous stress distributions.

Because the elastomer usually has excellent response properties, boundary stress microscopy is particularly useful for observing local stresses that can vary over many orders of magnitudes. For instance, it has been used to show that in a collagen I gel, the local stress can exceed average stresses by an order of magnitude, with a length scale that is much larger than the fiber mesh [123••]. Furthermore, boundary stress microscopy has revealed dramatic spatial and temporal stress fluctuations in shear thickening suspensions. This evidence suggests that a shear thickening sample spontaneously and intermittently separates into different fluid phases with significantly different properties [124••].

3.3. Phonon mode measurements

While vibrational modes in colloidal crystals can be heavily damped by the surrounding solvent [138–141], it has been recently proposed that suspensions can still be used as a "shadow system" for calculating the properties of glassy systems. The idea is to start with the particle positions and to calculate the vibrational modes as though the particles were in a simple harmonic potential [125,126,129]. Using a normal mode analysis, the displacement covariance matrices of the particles are diagonalized to obtain the normal modes (Fig. 2c). Some numerical and experimental studies have extended the principal of density of state measurement to correlate the soft spots – regions with concentrated low-frequency vibrational modes – to the shear transformation zones and defects in glasses [127,142,143] and crystals [128,144], respectively. This analysis technique is particularly interesting since it represents a hybrid approach that combines experiments and simulations.

3.4. Microrheology

Mechanical rheometry is a long-standing standard method used to characterize the flow behavior of complex materials. However, conventional rheological measurements have several critical limitations, such as the need for relatively large sample volumes (on the order of a milliliter), the inability to characterize local mechanical heterogeneity, and low probing frequency due to instrument inertia. In the last few decades, microrheology has been developed and become a popular tool to overcome these challenges. In the original papers of microrheology [145,146], Mason and Weitz tracked the trajectories of the tracer particles in various of complex fluids, determined their mean square displacement (MSD), and, via the Stokes-Sutherland-Einstein relation, determined the material's complex modulus. While in principal, any methods that measure the particle MSD (*e.g.* Diffusing wave spectroscopy, dynamic light scattering, and fluorescence correlation spectroscopy) can be used for conducting microrheology, direct imaging has the advantage of providing valuable information about the spatial distribution of mechanical heterogeneity. Modern implementations of direct imaging include both measurement of tracer particle motions and differential dynamic microscopy [147•,148••,149].

Over time, many important improvements have been made. For example, two-point microrheology has been introduced to mitigate the artifacts arising from the tracer shape and size dependencies, as well as the coupling between the tracer and its embedded medium [150]. Optical tweezers [131], magnetic

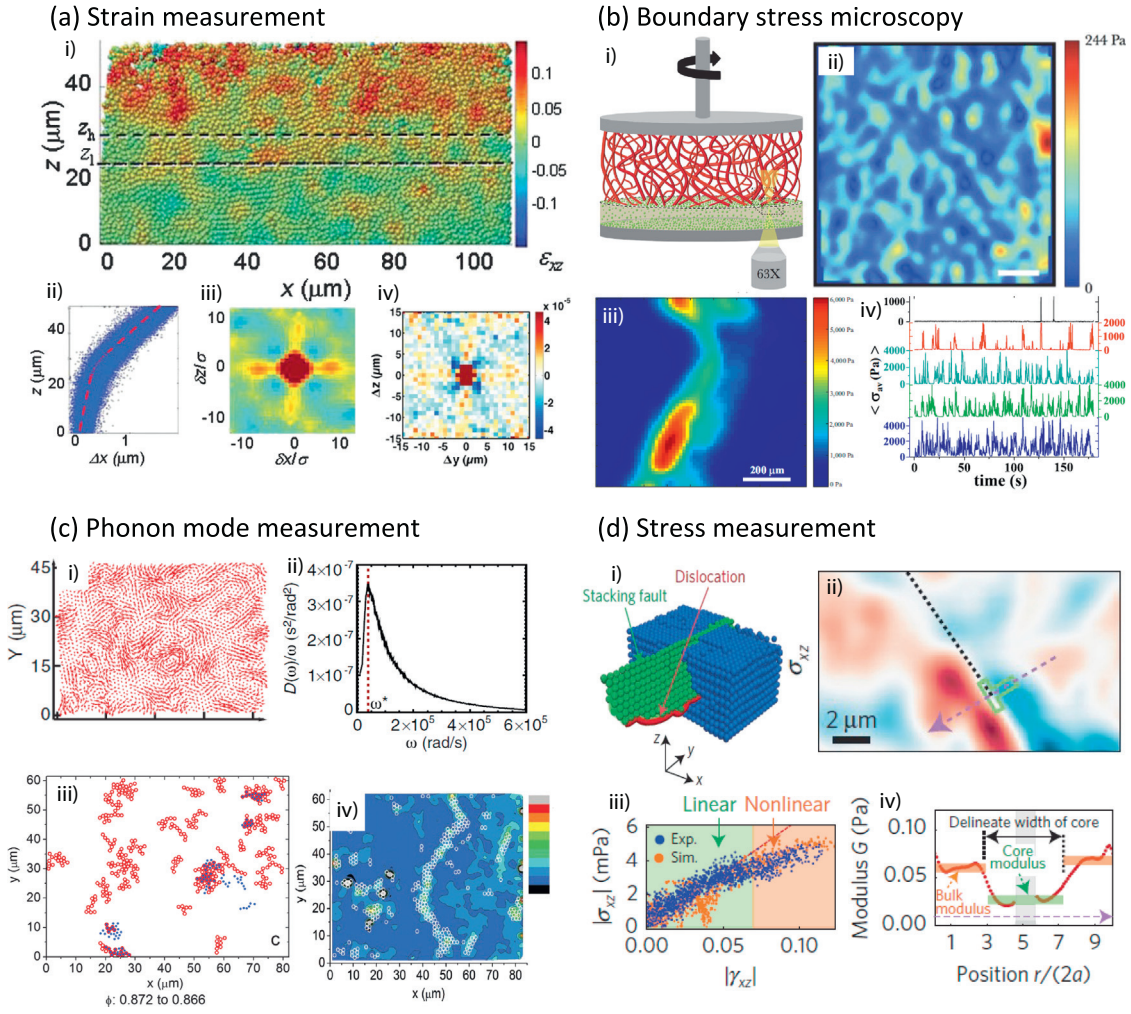

Fig. 2 Examples of mechanical measurements in colloidal suspensions: (a) i) Strain measurements show the shear banding behavior (red particles) in a sheared colloidal glass, as shown by the shear profile in ii) [121]. iii) The auto-correlation of the strain field exhibits a quadrupole pattern [121], consistent with the Eshelby inclusion model. iv) Surprisingly, similar correlation pattern has been found in quiescent colloidal glasses as well, suggesting that the thermal fluctuation can already trigger local structural transformations [122]. (b) i) Schematic of a boundary stress microscopy setup, where the bottom transparent plate is coated with a elastomer layer that contains tracer micro-particles [123••]. ii) stress heterogeneities measured in a collagen I sample [123••]. Spatial iii) and iv) temporal fluctuations of stresses in shear thickening suspensions [130•]. (c) i) Phonon mode measurements visualizes the normal mode in a colloidal glass [125]. ii) The measured density of state shows a clear boson peak feature [126]. iii) Soft spots determined using the phone mode method in a sheared colloidal glass [127] and iv) a quiescent polycrystal [128]. (d) i) and ii) Stress field surrounding a dislocation measured by SALSA [4••]. iii) and iv) by combining SALSA with the strain measurement, the local plasticity and modulus around the defect can be determined [4••].

fields [132], and atomic force microscopes [130•], have been implemented to drag tracers with forces much greater than thermal fluctuations, reaching the nonlinear response regime. In particular, to correctly link the measured nonlinear response to sample moduli, numerical models have been carried out to understand how the probe particle perturbs the sample's microstructure leading to corrections to the Stokes mobility [151–156]. Importantly, better particle location as described in Section 2 would improve these methods.

3.5. Local stress measurements

Another exciting development for measuring stresses in dense suspensions arises from adopting Irving and Kirkwood's idea [157], that determining forces is straightforward if the particle positions and interparticle potentials are known exquisitely. In particular, by summing the forces from neighboring particles one can determine the total force acting on any particle. This force distribution can then be smoothed

to determine the local stress. The situation is a bit more complicated for hard spheres since they only interact when particles collide with one another. Brady theoretically derived a formula to predict stresses in hard sphere suspensions based on calculation of the system averaged pair correlation function $g(\vec{r})$ [158]. The calculation relates the anisotropic particle distribution as measured by $g(\vec{r})$ to the suspension stress tensor. In 2010, Gao et al. [49] partially adopted this approach to experiments by measuring the pair correlation functions for flowing suspensions and comparing them to Stokesian Dynamics simulations. In 2011, Cheng et al. [48] implemented Brady's approach in full and showed that with experiments alone it is possible to extract the bulk stress from the pair correlation functions. This technique has gained rapid acceptance in the colloid community and is now implemented routinely by numerous groups [38,159,160].

In 2016, Lin et al. showed this macroscopic approach, can be generalized to the particle level. In particular, Stress Assessment from Local Structural Anisotropy (SALSA) measures the orientation distribution and probability of pairwise collisions between a particle and its nearest neighbors to determine the stresses arising from thermal collisions [4••]. SALSA has already been used to visualize the stress distributions surrounding crystal defects [4••] (See Fig. 2d) and the evolution of stresses in crystals under compression [78••]. Furthermore, SALSA has also been used to determine the viscosity of quiescent colloidal liquids by simply measuring thermally induced fluctuations of the shear stress [120•]. While current implementations have been used to investigate suspensions in the Brownian or low Péclet regime, it is likely that such measurements will also inform measurements of stress distributions under higher shear rates.

In Table 2 we provide a comparison of the range of techniques available for measuring forces. Once again, rather than a complete list, this table is meant to highlight the range of exciting techniques available for studying the heterogeneous mechanics in dense suspensions.

4. Application of analysis techniques to address long standing challenges in colloid science

The most exciting aspect of these novel analyses is the avenues that they open for investigating some of the most difficult problems in the science of suspension behaviors. Here, we sketch approaches for moving forward on a few of the science questions relating to crystals, glasses, gels, and shear thickening suspensions.

4.1. Crystals

Because of the relatively slow time scales associated with the particle motions, colloidal suspensions have been a valuable system for investigating a range of crystallization phenomena. In entropic crystals alone, these phenomena range from epitaxial growth [12,18] to defect nucleation and growth [13,63,161]. As colloidal systems become more sophisticated with different particle shapes [54,162] and tunable interparticle potentials [19–30] understanding how the energetic driving forces alter rates of various processes will become increasingly important for making progress. Already, techniques for inferring local strains are making valuable contributions related to the role of substrate curvature to crystallization [3,163,164]. Local stress measurements have already shown the importance of nonlinear stresses surrounding defects [4••] and the role that squeeze flows induced by increased confinement have on the stress distribution in colloidal crystals [78••]. It is entirely conceivable that such measurements can also be used to determine the role of nonlinear stresses in driving defect dynamics, an exciting prospect for scientists hoping to develop design principles for guiding defect nucleation, propagation, and coalescence.

The ability to measure variations in particle radii presents another fascinating direction for studying the phase separation or crystallization of one particle species in the presence of another impurity or secondary phase. Already, it has been shown that for a nearly monodisperse suspensions, even slightly smaller particles end up accumulating at the boundaries of crystal grains [3] and that a low concentration of impurities can substantially alter crystallization [165]. The ability to determine the 3D position and size of a large number of secondary particles opens the door to investigations of how a secondary phase and the stresses it generates alter crystallization pathways and resulting kinetics, an increasingly important problem for which relatively few model systems exist [166].

4.2. Glasses

Colloids have been a cornerstone model system for investigating glassy phenomena. They have been instrumental in verifying concepts ranging from dynamic heterogeneity and cage hopping [42,44], to identifying soft spots associated with low order normal modes [127,142,143] and long range strain correlations associated with yielding [121,122,136]. Moving forward, there are many avenues for improving measurement techniques to usher in an understanding of glasses at "the next decimal place." For example, most of the studies in colloidal glasses have been conducted with density-quenched monodisperse particles. This choice of system has been primarily dictated by experimental necessity – until recently it has been difficult to extract particle locations and sizes from images of dense polydisperse suspensions. But monodisperse suspensions locally crystallize, which makes them far from ideal for studying glassy behavior. The new inference techniques described in Table 1 now make it possible to easily investigate phenomena in bidisperse [3,46,167] and polydisperse suspensions [2••,3,101,112], determine volume fractions to much greater precision [2••], and even determine inhomogeneities in cage structure, which could elucidate whether the liquid to glass transition in colloids has the form of a Gardner transition with an increasingly fractal energy basin [168].

Additionally, much of the dynamic analysis of yielding in glassy suspensions has focused on measuring the magnitude

Table 2 Image-based methods for measuring mechanical properties of soft materials.

	Strain	Boundary stress	Phonon modes	Microrheology	Stress measurements (SALSA)
Mechanisms	Particle displacements	Tracers embedded in elastomer	Particle positions for calculating vibration modes	Passive: tracer's mean square displacement; Active: tracer's drag force	Inter-particle collision rate
Instrument modification	No	Elastomer coated on bottom substrate	No	Passive: no; Active: external field	No
Analysis challenges	Cannot infer nonlinear stress	Only shows stresses on the sample boundary; resolution bounded by tracer density	Requires long-time average to determine equilibrium positions; systematic errors from finite statistics [128]	Active: requires theoretical models for accurately interpreting nonlinear responses	Particle potential and collision criteria need careful validation
Sample limitation	Colloidal suspensions; only crystals allow force inferences relative to an undeformed lattice	None	None	Passive and active: tracer size must be taken into account	Inter-particle potential must be considered
Scientific finding examples	Shear transformation zones in colloidal glasses [47]; colloidal crystal defect nucleation dynamics [63]	Boundary stress inhomogeneities in shear thickening suspensions [124••] and bio-gels [123••]	Boson peaks and soft spots in colloidal glasses [125,127,129]	Passive and active: alternative method to rheometry for testing samples with small volume [130•,131,132]	Visualizing nonlinear stresses surrounding colloidal crystal defects [4••]

of and correlations in local relative strains [133]. Since there is no underlying lattice, it is not possible to define a strain in disordered suspensions. As such it is also not possible to determine whether the observed relative strains are relaxing or concentrating stresses. However, it should be possible to use techniques like boundary stress microscopy and SALSA to measure inhomogeneous stress distributions in sheared glasses and determine how they change under yielding. There are, of course, hurdles that remain. For example, the biggest difficulty with SALSA in a size-polydisperse suspension is to measure the particle positions and sizes with sufficient precision to accurately determine particle collisions probabilities. However, this particular hurdle can now be overcome by techniques like PERI. With such hurdles resolved, it should now be possible to observe how local stresses rearrange and percolate to enable the observed shear banding in yielding glasses [47].

4.3. Gels

Many of these improvements in measurement can also be applied to investigations of colloidal gels. In particular, analyses in Table 1 can be used to track gels made out of polydisperse particles. Additionally, PERI can be used in conjunction with simulations to extract nm scale interparticle potentials [2••]. This enables the use of SALSA for measuring the individual particle stresses in colloidal gel networks with depletion or DLVO interparticle potentials. For the first time, we will be able to image and statistically catalog the percentage of structurally necessary force chains versus redundant internal force loops [169]. In combination with boundary stress microscopy it should be possible to determine how the structurally necessary boundary forces distribute within the bulk of the gel. This combination of measurements would garner a substantially deeper understanding of how the local structure of gels dictates their loading, yielding, and flow response.

Recently, excitement surrounding colloidal gel behavior has focused on the ability to embed a system-wide memory using oscillatory shearing protocols. By applying a given oscillatory strain, one can repeatedly break and reform the gel network until it can withstand a particular strain [170•,171]. Measurements of local force inhomogeneities would also enable us to go much further in differentiating the properties associated with different regions of the gel responsible for maintaining rigidity versus those that enable plasticity and breakage. A

better understanding of these mechanisms will enable the formation of gels with properties that can be designed through various shear protocols.

4.4. Shear thickening

Colloidal suspensions also serve as an important model system for investigating non-Newtonian flows. These rheological phenomena include shear thickening at high strain rates, shear jamming of high suspension concentrations under rapid extensions, and solidification under rapid compression. There are many challenges in elucidating the microscopic origin for these behaviors. In shear thickening alone, there has been a vigorous and healthy debate relating to whether hydrodynamic or effective contact interactions between particles generate such behaviors [50,172–176•,177•]. Here too, the analyses we have described could play an important role in resolving such controversies. For example, using SALSA in combination with force-sensitive dyes [77] it may be possible to determine the net force on a particle due to contact interactions. Alternatively, PERI could be used to determine interactions due to charge repulsion enabling measurement of effective contacts between particles. These contact and effective contact interactions are thought by many to determine shear thickening behavior in suspensions. The analyses described here would enable a more rigorous testing of these ideas. On larger length scales boundary stress microscopy is being used to identify phase inhomogeneities in shear-thickened suspensions [124••]. As the shear rate increases, the suspension forms regions of thickened material that grow in size, coalesce, and eventually take over the entire suspension. Such measurements illustrate the rich physics that must be understood on intermediate length scales in order to achieve sufficient understanding of these behaviors.

4.5. "... a new discovery is likely to be found lurking in the next decimal place"

The scientific problems and methodologies we have sketched here to address them are only a small taste of the new mysteries and scientific tool box developments to come. As new analyses are developed to complement the rapid expansion of microscope capabilities, it is likely that new science will be discovered, and with it new problems to address. One final idea that we would like to put forth is that future techniques will most likely make even more use of computation – not just to analyze images, but as an additional tool for experiments. For instance, in SALSA computation is used to infer stresses based on estimation of interparticle collision probabilities. In phonon mode measurements, the colloidal suspension merely serves as a starting point for generating a computational model of a "shadow system." And cheap computation can be used not only to generate model fits to images, as in PERI, but also to interpret the experimental data, such as fitting experimental data with a complete simulation to extract interparticle potentials [2••]. Such trends foreshadow an increasingly rich range of creative approaches for making discoveries at "the next decimal place" of colloid science.

We thank Eric Weeks, Vinothan Manoharan, Roseanna Zia, and Mathieu Leocmach for helpful conversations in preparing this manuscript. This work was supported in part by National Science Foundation (NSF) Grant No. DMR-1507607 (I. C.), NSF Grant No. CBET-1509308 (N. L.), and ACS Grant No. PRF 56046-ND7 (B. L.).

References and recommended reading•,••

[1] Perrin J. La loi de stokes et le mouvement brownien. Compt Rendus 1908;147:475–6.
[2••] Bierbaum M, Leahy BD, Alemi AA, Cohen I, Sethna JP. Light microscopy at maximal precision. Phys Rev X 2017;7(4):041007. Parameter Estimation from Reconstruction of Images: Showed that it is possible to extract colloid particle position and size from an image at the information theoretic limit.
[3] Kurita R, Ruffner DB, Weeks ER. Measuring the size of individual particles from three-dimensional imaging experiments. Nat Commun 2012;3 [ncomms2114].
[4••] Lin NY, Bierbaum M, Schall P, Sethna JP, Cohen I. Measuring nonlinear stresses generated by defects in 3d colloidal crystals. Nat Mater 2016;15(11):1172–6. SALSA: Showed how to image forces at the single particle scale.
[5] Richtmyer F. The romance of the next decimal place. Science 1932;75(1931):1–5.
[6] Pieranski P, Strzelecki L, Pansu B. Thin colloidal crystals. Phys Rev Lett 1983;50(12):900.
[7] Pieranski P. Colloidal crystals. Contemp Phys 1983;24(1):25–73.
[8] Pieranski P. Two-dimensional interfacial colloidal crystals. Phys Rev Lett 1980;45(7):569.
[9] Pusey PN, Van Megen W. Phase behaviour of concentrated suspensions of nearly hard colloidal spheres. Nature 1986;320(6060):340–2.
[10] Sirota E, Ou-Yang H, Sinha S, Chaikin P, Axe J, Fujii Y. Complete phase diagram of a charged colloidal system: a synchro-tron X-ray scattering study. Phys Rev Lett 1989;62(13):1524.
[11] Murray CB, Kagan C, Bawendi M. Synthesis and characterization of monodisperse nanocrystals and close-packed nanocrystal assemblies. Annu Rev Mater Sci 2000;30(1):545–610.
[12] Van Blaaderen A, Ruel R, Wiltzius P, et al. Template-directed colloidal crystallization. Nature 1997;385(6614):321–4.
[13] Schall P, Cohen I, Weitz DA, Spaepen F. Visualization of dislocation dynamics in colloidal crystals. Science 2004;305(5692):1944–8.
[14] Yethiraj A, van Blaaderen A. A colloidal model system with an interaction tunable from hard sphere to soft and dipolar. Nature 2003;421(6922):513–7.
[15] Asakura S, Oosawa F. On interaction between two bodies immersed in a solution of macromolecules. J Chem Phys 1954;22(7):1255–6.
[16] Asakura S, Oosawa F. Interaction between particles suspended in solutions of macromolecules. J Polym Sci A Polym Chem 1958;33(126):183–92.

• of special interest.
•• of outstanding interest.

[17] Lekkerkerker H, Poon W-K, Pusey P, Stroobants A, Warren P. Phase behaviour of colloid+ polymer mixtures. Europhys Lett 1992;20(6):559.
[18] Lin K-h, Crocker JC, Prasad V, Schofield A, Weitz DA, Lubensky T, Yodh A. Entropically driven colloidal crystallization on patterned surfaces. Phys Rev Lett 2000;85(8):1770.
[19] Ganapathy R, Buckley MR, Gerbode SJ, Cohen I. Direct measurements of island growth and step-edge barriers in colloidal epitaxy. Science 2010;327(5964):445–8.
[20] Wang Y, Wang Y, Breed DR, Manoharan VN, Feng L, Hollingsworth AD, Weck M, Pine DJ. Colloids with valence and specific directional bonding. Nature 2012;491(7422):51–5.
[21] Leunissen ME, Christova CG, Hynninen A-P, Royall CP, Campbell AI, Imhof A, Dijkstra M, Van Roij R, Van Blaaderen A. Ionic colloidal crystals of oppositely charged particles. Nature 2005;437(7056):235–40.
[22] Shevchenko EV, Talapin DV, Kotov NA, O'brien S, Murray CB. Structural diversity in binary nanoparticle superlattices. Nature 2006;439(7072):55–9.
[23] Kalsin AM, Fialkowski M, Paszewski M, Smoukov SK, Bishop KJ, Grzybowski BA. Electrostatic self-assembly of binary nanoparticle crystals with a diamond-like lattice. Science 2006;312(5772):420–4.
[24] Erb RM, Son HS, Samanta B, Rotello VM, Yellen BB. Magnetic assembly of colloidal superstructures with multipole symmetry. Nature 2009;457(7232):999–1002.
[25] Yellen BB, Hovorka O, Friedman G. Arranging matter by magnetic nanoparticle assemblers. Proc Natl Acad Sci U S A 2005;102(25):8860–4.
[26] Bacri J-C, Perzynski R, Cabuil V, Massart R. Phase diagram of an ionic magnetic colloid: experimental study of the effect of ionic strength. J Colloid Interface Sci 1989;132(1):43–53.
[27] Mirkin CA, Letsinger RL, Mucic RC, Storhoff JJ. A DNA-based method for rationally assembling nanoparticles into macroscopic materials. Nature 1996;382(6592):607–9.
[28] Biancaniello PL, Kim AJ, Crocker JC. Colloidal interactions and self-assembly using DNA hybridization. Phys Rev Lett 2005;94(5):058302.
[29] Rogers WB, Shih WM, Manoharan VN. Using DNA to program the self-assembly of colloidal nanoparticles and microparticles. Nat Rev Mater 2016;1:16008.
[30] Wang Y, Jenkins IC, McGinley JT, Sinno T, Crocker JC. Colloidal crystals with diamond symmetry at optical lengthscales. Nat Commun 2017;8:14173.
[31] Paxton WF, Kistler KC, Olmeda CC, Sen A, Angelo SKSt, Cao Y, Mallouk TE, Lammert PE, Crespi VH. Catalytic nanomotors: autonomous movement of striped nanorods. J Am Chem Soc 2004;126(41):13424–31.
[32] Wang W, Duan W, Ahmed S, Mallouk TE, Sen A. Small power: autonomous nano-and micromotors propelled by self-generated gradients. Nano Today 2013;8(5):531–54.
[33] Palacci J, Sacanna S, Steinberg AP, Pine DJ, Chaikin PM. Living crystals of light-activated colloidal surfers. Science 2013;339(6122):936–40.
[34] Palacci J, Sacanna S, Kim S-H, Yi G-R, Pine D, Chaikin P. Light-activated self-propelled colloids. Phil Trans R Soc A 2014;372(2029):20130372.
[35] Ginot F, Theurkauff I, Levis D, Ybert C, Bocquet L, Berthier L, Cottin-Bizonne C. Nonequilibrium equation of state in suspensions of active colloids. Phys Rev X 2015;5(1):011004.
[36] Niu R, Palberg T, Speck T, et al. Self-assembly of colloidal molecules due to self-generated flow. Phys Rev Lett 2017;119(2):028001.
[37] Aarts DG, Lekkerkerker HN, Guo H, Wegdam GH, Bonn D. Hydrodynamics of droplet coalescence. Phys Rev Lett 2005;95(16):164503.
[38] Lin NY, Goyal S, Cheng X, Zia RN, Escobedo FA, Cohen I. Far-from-equilibrium sheared colloidal liquids: disentangling relaxation, advection, and shear-induced diffusion. Phys Rev E 2013;88(6):062309.
[39] Aarts DG, Schmidt M, Lekkerkerker HN. Direct visual observation of thermal capillary waves. Science 2004;304(5672):847–50.
[40] Lu PJ, Conrad JC, Wyss HM, Schofield AB, Weitz DA. Fluids of clusters in attractive colloids. Phys Rev Lett 2006;96(2):028306.
[41] Dibble CJ, Kogan M, Solomon MJ. Structure and dynamics of colloidal depletion gels: coincidence of transitions and heterogeneity. Phys Rev E 2006;74(4):041403.
[42] Kegel WK, van Blaaderen A. Direct observation of dynamical heterogeneities in colloidal hard-sphere suspensions. Science 2000;287(5451):290–3.
[43] van Blaaderen A, Wiltzius P. Real-space structure of colloidal hard-sphere glasses. Science 1995;270(5239):1177–9.
[44] Weeks ER, Crocker JC, Levitt AC, Schofield A, Weitz DA. Three-dimensional direct imaging of structural relaxation near the colloidal glass transition. Science 2000;287(5453):627–31.
[45] Pham K, Petekidis G, Vlassopoulos D, Egelhaaf S, Poon W, Pusey P. Yielding behavior of repulsion-and attraction-dominated colloidal glasses. J Rheol 2008;52(2):649–76.
[46] Yunker P, Zhang Z, Aptowicz KB, Yodh AG. Irreversible rearrangements, correlated domains, and local structure in aging glasses. Phys Rev Lett 2009;103(11):115701.
[47] Schall P, Weitz DA, Spaepen F. Structural rearrangements that govern flow in colloidal glasses. Science 2007;318(5858):1895–9.
[48] Cheng X, McCoy JH, Israelachvili JN, Cohen I. Imaging the microscopic structure of shear thinning and thickening colloidal suspensions. Science 2010;333:1276.
[49] Gao C, Kulkarni S, Morris J, Gilchrist J. Direct investigation of anisotropic suspension structure in pressure-driven flow. Phys Rev E 2010;81(4):041403.
[50] Ramaswamy M, Lin NY, Leahy BD, Ness C, Fiore AM, Swan JW, Cohen I. How confinement-induced structures alter the contribution of hydrodynamic and short-ranged repulsion forces to the viscosity of colloidal suspensions. Phys Rev X 2017;7(4):041005.
[51] Glotzer SC, Solomon MJ. Anisotropy of building blocks and their assembly into complex structures. Nat Mater 2007;6:557.
[52] Mohraz A, Solomon MJ. Direct visualization of colloidal rod assembly by confocal microscopy. Langmuir 2005;21(12):5298–306.
[53] Kraft DJ, Groenewold J, Kegel WK. Colloidal molecules with well-controlled bond angles. Soft Matter 2009;5(20):3823–6.
[54] Lee SH, Gerbode SJ, John BS, Wolfgang AK, Escobedo FA, Cohen I, Liddell CM. Synthesis and assembly of nonspherical hollow silica colloids under confinement. J Mater Chem 2008;18:4912.
[55] Sacanna S, Irvine W, Chaikin PM, Pine DJ. Lock and key colloids. Nature 2010;464(7288):575–8.
[56] Hernandez CJ, Mason TG. Colloidal alphabet soup: monodisperse dispersions of shape-designed lithoparticles. J Phys Chem C 2007;111(12):4477–80.

[57] Zhao K, Mason TG. Frustrated rotator crystals and glasses of brownian pentagons. Phys Rev Lett 2009;103(20):208302.
[58] Badaire S, Cottin-Bizonne C, Woody JW, Yang A, Stroock AD. Shape selectivity in the assembly of lithographically designed colloidal particles. J Am Chem Soc 2007;129(1):40–1.
[59] Rolland JP, Maynor BW, Euliss LE, Exner AE, Denison GM, DeSimone JM. Direct fabrication and harvesting of monodisperse, shape-specific nanobiomaterials. J Am Chem Soc 2005;127(28):10096–100.
[60] Damasceno PF, Engel M, Glotzer SC. Predictive self-assembly of polyhedra into complex structures. Science 2012;337(6093):453–7.
[61] Praad V, Semwogerere D, Weeks ER. Confocal microscopy of colloids. J Phys Condens Matter 2007;19:113102.
[62] Gasser U, Weeks ER, Schofield A, Pusey P, Weitz D. Real-space imaging of nucleation and growth in colloidal crystallization. Science 2001;292(5515):258–62.
[63] Schall P, Cohen I, Weitz DA, Spaepen F. Visualizing dislocation nucleation by indenting colloidal crystals. Nature 2006;440(7082):319–23.
[64] Savage J, Dinsmore A. Experimental evidence for two-step nucleation in colloidal crystallization. Phys Rev Lett 2009;102(19):198302.
[65] Savage JR, Hopp SF, Ganapathy R, Gerbode SJ, Heuer A, Cohen I. Entropy-driven crystal formation on highly strained substrates. Proc Natl Acad Sci 2013;110(23):9301–4.
[66] Crocker JC, Grier DG. Methods of digital video microscopy for colloidal studies. J Colloid Interface Sci 1995;179:298.
[67] Jenkins MC, Egelhaaf SU. Confocal microscopy of colloidal particles: towards reliable, optimum coordinates. Adv Colloid Interface Sci 2008;136(1):65–92.
[68] Jensen KE, Nakamura N. Note: an iterative algorithm to improve colloidal particle locating. Rev Sci Instrum 2016;87(6):066103. Showed how to get all particles using Crocker-Grier algorithm.
[69] Israelachvili J, Tabor D. The measurement of van der Waals dispersion forces in the range 1.5 to 130 nm 331; 1972; 19–38.
[70] Crocker JC, Grier DG. Microscopic measurement of the pair interaction potential of charge-stabilized colloid. Phys Rev Lett 1994;73(2):352.
[71] Trefalt G, Behrens SH, Borkovec M. Charge regulation in the electrical double layer: ion adsorption and surface interactions. Langmuir 2015;32(2):380–400.
[72] Crocker JC, Matteo J, Dinsmore A, Yodh A. Entropic attraction and repulsion in binary colloids probed with a line optical tweezer. Phys Rev Lett 1999;82(21):4352.
[73] Mukhija D, Solomon MJ. Translational and rotational dynamics of colloidal rods by direct visualization with confocal microscopy. J Colloid Interface Sci 2007;314:98–106.
[74] Besseling TH, Hermes M, Kuijk A, de Nijs B, Deng T-S, Dijkstra M, Imhof A, van Blaaderen A. Determination of the positions and orientations of concentrated rod-like colloids from 3d microscopy data. J Phys Condens Matter 2015;27:194109. Showed how to feature rods.
[75] Conley GM, Nöjd S, Braibanti M, Schurtenberger P, Scheffold F. Superresolution microscopy of the volume phase transition of pnipam microgels. Colloids Surf A Physicochem Eng Asp 2016;499:18–23. Use of PALM to image NIPA microparticles.
[76] Conley GM, Aebischer P, Nöjd S, Schurtenberger P, Scheffold F. Jamming and overpacking fuzzy microgels: Deformation, interpenetration, and compression. Sci Adv 2017;3(10):e1700969.
[77] Suhina T, Weber B, Carpentier CE, Lorincz K, Schall P, Bonn D, Brouwer AM. Fluorescence microscopy visualization of contacts between objects. Angew Chem Int Ed 2015;54(12):3688–91.
[78] Lin NY, Cohen I. Relating microstructure and particle-level stress in colloidal crystals under increased confinement. Soft Matter 2016;12(44):9058–67. Application of SALSA to understand stresses induced by applying squeeze flow to a crystal.
[79] Betzig E, et al. Imaging intracellular fluorescent proteins at nanometer resolution. Science 2006;313:1642–5.
[80] Rust MJ, Bates M, Zhuang X. Sub-diffraction-limit imaging by stochastic optical reconstruction microscopy (storm). Nat Methods 2006;3:793.
[81] Hell SW, Wichmann J. Breaking the diffraction resolution limit by stimulated emission: stimulated-emission-depletion fluorescence microscopy. Opt Lett 1994;19:780.
[82] Kner P, Chhun BB, Griffis ER, Winoto L, Gustafsson MGL. Super-resolution video microscopy of live cells by structured illumination. Nat Methods 2009;6:339–42.
[83] Chen B-C, Legant WR, Wang K, Shao L, Milkie DE, Davidson MW, Janetopoulos C, Wu XS, Hammer JA, Liu Z, et al. Lattice light-sheet microscopy: imaging molecules to embryos at high spatiotemporal resolution. Science 2014;346(6208):1257998.
[84] Snoeyink C, Wereley S. A novel 3d3c particle tracking method suitable for microfluidic flow measurements. Exp Fluids 2013;54(1):1453.
[85] Gabor D. A new microscopic principle. Nature 1948;161:777–8.
[86] Gabor D, et al. Microscopy by reconstructed wave-fronts 197(1051); 1949; 454–87.
[87] Sheng J, Malkiel E, Katz J. Digital holographic microscope for measuring three-dimensional particle distributions and motions. Appl Optics 2006;45(16):3893–901.
[88] Lee S-H, Grier DG. Holographic microscopy of holographically trapped three-dimensional structures. Opt Express 2007;15(4):1505–12.
[89] Lee S-H, Roichman Y, Yi G-R, Kim S-H, Yang S-M, Van Blaaderen A, Van Oostrum P, Grier DG. Characterizing and tracking single colloidal particles with video holographic microscopy. Opt Express 2007;15(26):18275–82.
[90] Cheong FC, Krishnatreya BJ, Grier DG. Strategies for three-dimensional particle tracking with holographic video microscopy. Opt Express 2010;18(13):13563–73.
[91] Dixon L, Cheong FC, Grier DG. Holographic deconvolution microscopy for high-resolution particle tracking. Opt Express 2011;19(17):16410–7.
[92] Dimiduk TG, Manoharan VN. Bayesian approach to analyzing holograms of colloidal particles. Opt Express 2016;24(21):24045–60. Applications of Bayesian techniques to analysis of suspension hologram images.
[93] Fung J, Martin KE, Perry RW, Kaz DM, McGorty R, Manoharan VN. Measuring translational, rotational, and vibrational dynamics in colloids with digital holographic microscopy. Opt Express 2011;19(9):8051–65.
[94] Fung J, Perry RW, Dimiduk TG, Manoharan VN. Imaging multiple colloidal particles by fitting electromagnetic scattering solutions to digital holograms. J Quant Spectrosc Radiat Transf 2012;113(18):2482–9.
[95] Fung J, Manoharan VN. Holographic measurements of anisotropic three-dimensional diffusion of colloidal clusters. Phys Rev E 2013;88(2):020302.
[96] Cheong FC, Grier DG. Rotational and translational diffusion of copper oxide nanorods measured with holographic video microscopy. Opt Express 2010;18(7):6555–62.

[97] Wang A, Dimiduk TG, Fung J, Razavi S, Kretzschmar I, Chaudhary K, Manoharan VN. Using the discrete dipole approximation and holographic microscopy to measure rotational dynamics of non-spherical colloidal particles. J Quant Spectrosc Radiat Transf 2014;146:499–509.
[98•] Cheong FC, Kasimbeg P, Ruffner DB, Hlaing EH, Blusewicz JM, Philips LA, Grier DG. Holographic characterization of colloidal particles in turbid media. Appl Phys Lett 2017;111(15):153702. Application of holographic imaging in turbid suspensions.
[99] Dimiduk TG, Kosheleva EA, Kaz D, McGorty R, Gardel EJ, Manoharan VN. A simple, inexpensive holographic microscope. Biomedical Optics, Optical Society of America; 2010. p. JMA38.
[100] Deegan RD, Bakajin O, Dupont TF, Huber G, Nagel SR, Witten TA. Capillary flow as the cause of ring stains from dried liquid drops. Nature 1997;389(6653):827–9.
[101] Leocmach M, Tanaka H. A novel particle tracking method with individual particle size measurement and its application to ordering in glassy hard sphere colloids. Soft Matter 2013;9(5):1447–57.
[102•] Dreyfus R, Xu Y, Still T, Hough LA, Yodh A, Torquato S. Diagnosing hyperuniformity in two-dimensional, disordered, jammed packings of soft spheres. Phys Rev E 2015;91(1):012302. Analysis of hyperuniformity in 2D suspensions.
[103] Crocker JC, Grier DG. Methods of digital video microscopy for colloidal studies. J Colloid Interface Sci 1996;179(1):298–310.
[104] Elliot MS, Poon WC. Conventional optical microscopy of colloidal suspensions. Adv Colloid Interface Sci 2001;92(1):133–94.
[105] Lu PJ, Shutman M, Sloutskin E, Butenko AV. Locating particles accurately in microscope images requires image-processing kernels to be rotationally symmetric. Opt Express 2013;21(25):30755–63.
[106] Gao Y, Kilfoil ML. Accurate detection and complete tracking of large populations of features in three dimensions. Opt Express 2009;17(6):4685–704.
[107] Berglund AJ, McMahon MD, McClelland JJ, Liddle JA. Fast, bias-free algorithm for tracking single particles with variable size and shape. Opt Express 2008;16(18):14064–75.
[108•] Burov S, Figliozzi P, Lin B, Rice SA, Scherer NF, Dinner AR. Single-pixel interior filling function approach for detecting and correcting errors in particle tracking. Proc Natl Acad Sci 2017;114(2):221–6. Demonstrated a approach for detecting and correcting errors in particle tracking.
[109] Pathasarathy R. Rapid, accurate particle tracking by calculation of radial symmetry centers. Nat Methods 2012;9:724–6.
[110] Mayoral K, Kennair TP, Zhu X, Milazzo J, Ngo K, Fryd MM, Mason TG. Rotational fourier tracking of diffusing polygons. Phys Rev E 2011;84(5):051405.
[111] Leahy B, Cheng X, Ong DC, Liddell-Watson C, Cohen I. Enhancing rotational diffusion using oscillatory shear. Phys Rev Lett 2013;110:228301.
[112] Brujić J, Edwards SF, Grinev DV, Hopkinson I, Brujić D, Makse HA. 3d bulk measurements of the force distribution in a compressed emulsion system. Faraday Discuss 2003;123:207–20.
[113] Jorjadze I, Pontani L-L, Brujic J. Microscopic approach to the nonlinear elasticity of compressed emulsions. Phys Rev Lett 2013;110(4):048302.
[114] Kurita R, Weeks ER. Incompressibility of polydisperse random-close-packed colloidal particles. Phys Rev E 2011;84(3):030401.
[115•] Heckendorf D, Mutch K, Egelhaaf S, Laurati M. Size-dependent localization in polydisperse colloidal glasses. Phys Rev Lett 2017;119(4):048003. Observed size-dependent localization in polydisperse glasses.
[116] D. B. Allan, T. A. Caswell, N. C. Keim, Trackpy v0.2 (May 2014). https://doi.org/10.5281/zenodo.9971. URL github.com/soft-matter/trackpy
[117] [link]. URL http://www.physics.emory.edu/faculty/weeks//idl/.
[118] https://doi.org/10.5281/zenodo.31286, [link]. URL https://doi.org/10.5281/zenodo.31286
[119] [link]. URL https://github.com/peri-source/peri.
[120•] Lin NY, Bierbaum M, Cohen I. Determining quiescent colloidal suspension viscosities using the green-kubo relation and image-based stress measurements. Phys Rev Lett 2017;119(13):138001. Analyzed thermal fluctuations in a quiescent suspension to determine the Brownian viscosity as a function of volume fraction.
[121] Chikkadi V, Wegdam G, Bonn D, Nienhuis B, Schall P. Long-range strain correlations in sheared colloidal glasses. Phys Rev Lett 2011;107(19):198303.
[122] Jensen K, Weitz DA, Spaepen F. Local shear transformations in deformed and quiescent hard-sphere colloidal glasses. Phys Rev E 2014;90(4):042305.
[123••] Arevalo RC, Kumar P, Urbach JS, Blair DL. Stress heterogeneities in sheared type-i collagen networks revealed by boundary stress microscopy. PLoS One 2015;10(3):e0118021. Used boundary stress to measure heterogeneities in sheared type-I collagen networks.
[124••] Rathee V, Blair DL, Urbach JS. Localized stress fluctuations drive shear thickening in dense suspensions. Proc Natl Acad Sci 2017;114(33):8740–5 [arXiv: http://www.pnas.org/content/114/33/8740.full.pdf, https://doi.org/10.1073/pnas.1703871114. URL http://www.pnas.org/content/114/33/8740.abstract]. Used boundary stress to measure heterogeneities in thickening suspension. Established a meso-scale phase separation during transition to thickened state.
[125] Kaya D, Green N, Maloney C, Islam M. Normal modes and density of states of disordered colloidal solids. Science 2010;329(5992):656–8.
[126] Chen K, Ellenbroek WG, Zhang Z, Chen DT, Yunker PJ, Henkes S, Brito C, Dauchot O, Van Saarloos W, Liu AJ, et al. Low-frequency vibrations of soft colloidal glasses. Phys Rev Lett 2010;105(2):025501.
[127] Chen K, Manning M, Yunker PJ, Ellenbroek WG, Zhang Z, Liu AJ, Yodh AG. Measurement of correlations between low-frequency vibrational modes and particle rearrangements in quasi-two-dimensional colloidal glasses. Phys Rev Lett 2011;107(10):108301.
[128] Chen K, Still T, Schoenholz S, Aptowicz KB, Schindler M, Maggs A, Liu AJ, Yodh A. Phonons in two-dimensional soft colloidal crystals. Phys Rev E 2013;88(2):022315.
[129] Ghosh A, Chikkadi VK, Schall P, Kurchan J, Bonn D. Density of states of colloidal glasses. Phys Rev Lett 2010;104(24):248305.
[130•] Rigato A, Miyagi A, Scheuring S, Rico F. High-frequency microrheology reveals cytoskeleton dynamics in living cells. Nat Phys, 13; 2017. p. 771–5. Application of microrheology to biopolymer-membrane complexes.
[131] Helfer E, Harlepp S, Bourdieu L, Robert J, MacKintosh F, Chatenay D. Microrheology of biopolymer-membrane complexes. Phys Rev Lett 2000;85(2):457.
[132] Amblard F, Maggs AC, Yurke B, Pargellis AN, Leibler S. Subdiffusion and anomalous local viscoelasticity in actin networks. Phys Rev Lett 1996;77(21):4470.

[133] Falk ML, Langer JS. Dynamics of viscoplastic deformation in amorphous solids. Phys Rev E 1998;57(6):7192.
[134•] Sussman DM, Schoenholz SS, Xu Y, Still T, Yodh A, Liu AJ. Strain fluctuations and elastic moduli in disordered solids. Phys Rev E 2015;92(2):022307. Analyzed a colloidal suspension as a shadow system to determine strain fluctuations and elastic moduli in disordered solids.
[135] Rahmani Y, Koopman R, Denisov D, Schall P. Visualizing the strain evolution during the indentation of colloidal glasses. Phys Rev E 2014;89(1):012304.
[136] Chikkadi V, Miedema D, Dang M, Nienhuis B, Schall P. Shear banding of colloidal glasses: observation of a dynamic first-order transition. Phys Rev Lett 2014;113(20):208301.
[137] Illing B, Fritschi S, Hajnal D, Klix C, Keim P, Fuchs M. Strain pattern in supercooled liquids. Phys Rev Lett 2016;117(20):208002.
[138] Cheng Z, Zhu J, Russel WB, Chaikin P. Phonons in an entropic crystal. Phys Rev Lett 2000;85(7):1460.
[139] Keim P, Maret G, Herz U, von Grünberg H-H. Harmonic lattice behavior of two-dimensional colloidal crystals. Phys Rev Lett 2004;92(21):215504.
[140] Baumgartl J, Dietrich J, Dobnikar J, Bechinger C, von Grünberg HH. Phonon dispersion curves of two-dimensional colloidal crystals: the wavelength-dependence of friction. Soft Matter 2008;4(11):2199–206.
[141] Ohshima YN, Nishio I. Colloidal crystal: bead–spring lattice immersed in viscous media. J Chem Phys 2001;114(19):8649–58.
[142] Ding J, Patinet S, Falk ML, Cheng Y, Ma E. Soft spots and their structural signature in a metallic glass. Proc Natl Acad Sci 2014;111(39):14052–6.
[143] Manning ML, Liu AJ. Vibrational modes identify soft spots in a sheared disordered packing. Phys Rev Lett 2011;107(10):108302.
[144] Rottler J, Schoenholz SS, Liu AJ. Predicting plasticity with soft vibrational modes: from dislocations to glasses. Phys Rev E 2014;89(4):042304.
[145] Mason TG, Weitz D. Optical measurements of frequency-dependent linear viscoelastic moduli of complex fluids. Phys Rev Lett 1995;74(7):1250.
[146] Mason T, Weitz D. Linear viscoelasticity of colloidal hard sphere suspensions near the glass transition. Phys Rev Lett 1995;75(14):2770.
[147•] Bayles AV, Squires TM, Helgeson ME. Dark-field differential dynamic microscopy. Soft Matter 2016;12(8):2440–52. Showed how to apply dark-field imaging ddm to extract displacements and relate these to stresses via microrheology.
[148••] Edera P, Bergamini D, Trappe V, Giavazzi F, Cerbino R, et al. Illustration of ddm approach to microrheology. Phys Rev Mater 2017;1(7):073804.
[149] Cerbino R, Trappe V. Differential dynamic microscopy: probing wave vector dependent dynamics with a microscope. Phys Rev Lett 2008;100(18):188102.
[150] Crocker JC, Valentine MT, Weeks ER, Gisler T, Kaplan PD, Yodh AG, Weitz DA. Two-point microrheology of inhomogeneous soft materials. Phys Rev Lett 2000;85(4):888.
[151] Zia RN. Active and passive microrheology: theory and simulation. Annu Rev Fluid Mech 2018;150:371–405.
[152] Khair AS, Brady JF. Single particle motion in colloidal dispersions: a simple model for active and nonlinear microrheology. J Fluid Mech 2006;557:73–117.
[153] Squires TM, Brady JF. A simple paradigm for active and nonlinear microrheology. Phys Fluids 2005;17(7):073101.
[154] Squires TM. Nonlinear microrheology: bulk stresses versus direct interactions. Langmuir 2008;24(4):1147–59.
[155] Zia RN, Brady JF. Single-particle motion in colloids: force-induced diffusion. J Fluid Mech 2010;658:188–210.
[156] Swan JW, Zia RN, Brady JF. Large amplitude oscillatory microrheology. J Rheol 2014;58(1):1–41.
[157] Irving J, Kirkwood JG. The statistical mechanical theory of transport processes. iv. The equations of hydrodynamics. J Chem Phys 1950;18(6):817–29.
[158] Brady JF. The rheological behavior of concentrated colloidal dispersions. J Chem Phys 1993;99:567.
[159] Xu B, Gilchrist JF. Microstructure of sheared monosized colloidal suspensions resulting from hydrodynamic and electrostatic interactions. J Chem Phys 2014;140(20):204903.
[160] Koumakis N, Laurati M, Jacob A, Mutch K, Abdellali A, Schofield A, Egelhaaf S, Brady J, Petekidis G. Start-up shear of concentrated colloidal hard spheres: stresses, dynamics, and structure. J Rheol 2016;60(4):603–23.
[161] Gerbode SJ, Lee SH, Liddell CM, Cohen I. Restricted dislocation motion in crystals of colloidal dimer particles. Phys Rev Lett 2008;101(5):058302.
[162] Rossi L, Sacanna S, Irvine WT, Chaikin PM, Pine DJ, Philipse AP. Cubic crystals from cubic colloids. Soft Matter 2011;7(9):4139–42.
[163] Irvine WT, Vitelli V, Chaikin PM. Pleats in crystals on curved surfaces. Nature 2010;468(7326):947–51.
[164] Meng G, Paulose J, Nelson DR, Manoharan VN. Elastic instability of a crystal growing on a curved surface. Science 2014;343(6171):634–7.
[165] de Villeneuve VW, Dullens RP, Aarts DG, Groeneveld E, Scherff JH, Kegel WK, Lekkerkerker HN. Colloidal hard-sphere crystal growth frustrated by large spherical impurities. Science 2005;309(5738):1231–3.
[166] De Yoreo JJ, Gilbert PU, Sommerdijk NA, Penn RL, Whitelam S, Joester D, Zhang H, Rimer JD, Navrotsky A, Banfield JF, et al. Crystallization by particle attachment in synthetic, biogenic, and geologic environments. Science 2015;349(6247):aaa6760.
[167] Nugent CR, Edmond KV, Patel HN, Weeks ER. Colloidal glass transition observed in confinement. Phys Rev Lett 2007;99(2):025702.
[168] Parisi G, Charbonneau P, Zamponi F, Urbani P, Kurchan J. Fractal free energy landscapes in structural glasses. Nat Commun 2014;5(5):3725.
[169] Maxwell JC. L. on the calculation of the equilibrium and stiffness of frames. London Edinb Dublin Philos Mag J Sci 1864;27(182):294–9.
[170•] Moghimi E, Jacob AR, Koumakis N, Petekidis G. Colloidal gels tuned by oscillatory shear. Soft Matter 2017;13(12):2371–83. Showed that the mechanical properties of colloidal gels can be tuned through application of oscillatory shear.
[171] Schwen E, Ramaswamay M, Jan L, Cheng C-M, Cohen I. Embedding memories in colloidal gels though oscillatory shear. Bull Am Phys Soc 2017;62.
[172] Wagner NJ, Brady JF. Shear thickening in colloidal dispersions. Phys Today 2009;62(10):27–32.
[173] Lootens D, Van Damme H, Hémar Y, Hébraud P. Dilatant flow of concentrated suspensions of rough particles. Phys Rev Lett 2005;95(26):268302.
[174] Seto R, Mari R, Morris JF, Denn MM. Discontinuous shear thickening of frictional hard-sphere suspensions. Phys Rev Lett 2013;111(21):218301.

[175] Brown E, Jaeger HM. Shear thickening in concentrated suspensions: phenomenology, mechanisms and relations to jamming. Rep Prog Phys 2014;77(4):046602.

[176•] Lin NY, Guy BM, Hermes M, Ness C, Sun J, Poon WC, Cohen I. Hydrodynamic and contact contributions to continuous shear thickening in colloidal suspensions. Phys Rev Lett 2015;115 (22):228304. Determined that contact or effective contact forces dominate shear thickening in silica and PMMA colloidal suspensions.

[177•] Lin NY, Ness C, Cates ME, Sun J, Cohen I. Tunable shear thickening in suspensions. Proc Natl Acad Sci 2016;113(39): 10774–8 [201608348]. Showed how to dethicken a suspension through application of orthogonal shear flows.